RSC Advances

ROYAL SOCIETY OF CHEMISTRY

www.rsc.org/advances

Effect of detonation polycrystalline diamond modification on thermal decomposition of RDX

Yi Tong,[a*] Rui Liu,[a,b] Tonglai Zhang[a]

A well-dispersed micron detonation polycrystalline diamond (DPD) was prepared and modified on RDX particles, preparing four DPD-modified RDX (DMR) composites with the modified amount increasing from 1/9 to 1/3. The modification effect on the thermal decomposition and kinetics of RDX were studied by dynamic pressure measuring thermal analysis (DPTA), differential scanning calorimetry (DSC) and thermogravimetric analysis (TG) techniques. As the modified amount increased, the gas emission, reaction rate constant, decomposition temperature, kinetic and thermodynamic parameters of the composites increased firstly and decreased afterwards. DPD had a catalytic effect on the thermal decomposition of RDX, but this effect was not in linear correlation with the modified amount. The DPD-modified amount of 1/7 had the optimal catalytical effect. Under the DPD modification less than 1/7, the thermal decomposition of RDX was accelerated by DPD. As the modified amount exceeded 1/7, the excessive DPD modification conversely hindered the decomposition of RDX. The thermal decomposition kinetics demonstrated that the thermal decompositions of DMRs conformed to the multi-step reaction mechanism involving the catalytic reaction and secondary reaction, while they had the same rate-determining step which is the scission of N-NO_2 bonds of RDX. The DPD modification change the reaction pathway and reaction rate to affect the decomposition mechanisms and kinetics.

[a] State Key Lab. of Explosion Science & Technology, School of Mechatronic Engineering, Beijing Institute of Technology. No.5, Zhongguancun South Street, Beijing, 100081, P. R. China. E-mail: tongyi@bit.edu.cn (corresponding author: Yi Tong)

[b] No.1 Institute of Design, China Wuzhou Engineering Group. No.85, Xibianmennei Street, Beijing, 100053, P. R. China

Introduction

Detonation polycrystalline diamond (DPD) is micron-sized synthetic diamond powder produced by graphite and explosive at detonation condition.[1] The naturally-formed diamond is the hardest and most abrasion resistant of all materials. The synthetic DPD inherits the superior properties of bulk diamond and delivers them at small scale. DPD has extreme hardness, wear resistance and thermal conductivity like diamond, additionally large surface effect and small scale effect like micron materials.[2-4] For above-mentioned advantages, DPD is a great material used for composite preparation, precision polishing, head processing for computer hard disk, and connector of optical fiber.[5, 6] As the development of micro- and nano technology, the composite modification using the ultrafine particles, such as graphene,[7, 8] carbon nanotube[9, 10] and detonation nanodiamond[11], is one of the most important techniques for preparation of the novel materials. Therefore, the ultrafine DPD can be applied to research and development of the modified composites.

Hexahydro-1,3,5-trinitro-l,3,5-triazine (RDX) is an important explosive and widely used in aviation, ordnance and mining industries.[12, 13] Development of the high-energy and low-sensitivity explosives has become a hot topic in recent years.[14] One of the most effective attempts is to design the composite explosives through adding the combustible, oxidizing, or energetic components.[15, 16] The ultrafine metal powders, such as Al, Cu and Ni, have shown great potential due to the high enthalpy release, high surface reactivity and density increase.[17-19] However, the metal powders tend to oxidize at worst to self-ignition, and cause heavy disaster as well as metal pollution and poor cost efficiency. The ultrafine DPD is modified on RDX, the composite is promising to exhibit some exceptional performances. However, so far the researches are seldom due to the potential explosion hazards and difficulties which lie in the fabrication process. In this work, four kinds of DPD-modified RDX (DMR) composites with different modified amounts were prepared, and the thermal decompositions and kinetics were studied by DPTA, DSC and TG techniques.

Experimental

Preparation of DPD micropowder

DPD was prepared by using the high-purity graphite powder and explosive as the starting materials, through the direct conversion of carbon source at the ultra-high pressure of more than 10 GPa, temperature of higher than 2000 °C. The high pressure and temperature were generated by the detonation of powerful explosive RDX or HMX in a non-oxidizing cooling medium. The chemical purification was treated by perchloric acid and sulfuric acid at the elevated temperature ~300 ^{o}C, when the condensed carbon was oxidized in liquid phase and the non-diamond structures decomposed gradually. The primary product was washed by deionized water, then filtrated and dried to obtain the gray-black powder. The powder was screened to obtain the refined DPD micropowder. The preparation process is shown in **Fig. 1**.

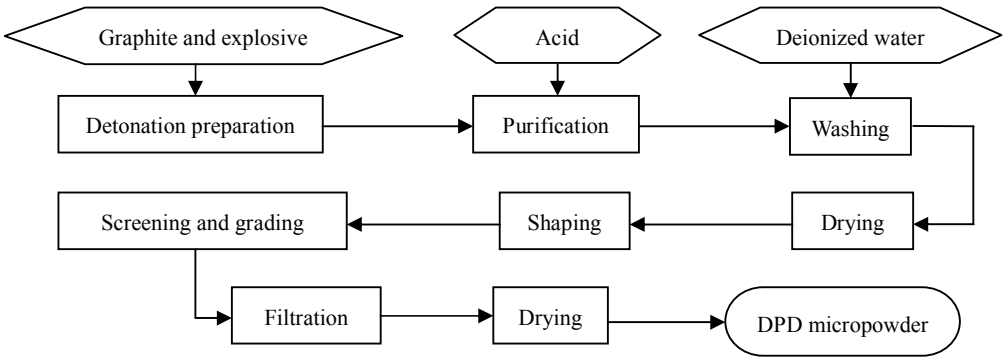

Fig. 1 Preparation process of DPD

Preparation of DMR composites

1 g RDX was dissolved in 100 mL acetone in 60 ^{o}C water bath under stirring. 0.5 g DPD was dispersed in 100 mL anhydrous ethanol with the aid of 0.10 mL surfactant sorbitan monooleate (Span-80). The solution was treated by ultrasonic oscillation for more than 1 hour until DPD was completely dispersed. The dispersion was put onto a magnetic stirring device and heated to 60 ^{o}C under 60 rpm stirring. Meanwhile, the pre-warm acetone solution in which RDX had been dissolved was added dropwise into the DPD dispersion. After dropping, the mixed solution was kept stirring for 30 minutes, then quickly transferred into a vacuum distillation flask and

distilled by using a rotary evaporator with the rotation speed of 45 rpm at 80 ^{o}C. After 80% solvent was evaporated, the remaining thick slurry was filtrated rapidly and washed by anhydrous ethanol and deionized water. The filter cake was dried at 40 ^{o}C over 24 hours, obtaining the gray-black powder. To determine the DPD-modified effect, four DMR composites with the different ratios of ingredients were prepared under the same experimental conditions. The ingredient ratios of DPD to RDX were designed to 1:8 (DMR1), 1:6 (DMR2), 1:4 (DMR3), and 1:2 (DMR4) which correspond to the increasing DPD-modified amounts of 1/9, 1/7, 1/5 and 1/3.

Apparatus and methods

Dynamic pressure measuring thermal analysis (DPTA) was used to study the initial thermal decomposition at constant temperature.[20] Sample was weighed (1.0000±0.0010) g and loaded in an explosion-proof glass test tube. The tube was sealed and evacuated, then put in to the thermostat, and hold at 100 ºC for 48 hours.

Thermogravimetric analysis (TG) and differential scanning calorimetry (DSC) were applied to study the complete thermal decomposition under linear heating. Pyris-1 TGA (Perkin-Elmer, USA) was employed with an unsealed platinum pan. Less than 0.5 mg of sample was heated from 50 ºC to 500 ºC at the rates of 5, 10, 15 and 20 ºC min^{-1} respectively. The atmosphere was high-pure nitrogen with the flowing rate of 20 mL min^{-1} under the pressure of 0.2 MPa. Pyris-1 DSC (Perkin-Elmer, USA) was used with an uncovered aluminum crucible. Less than 0.5 mg of sample was heated from 50 ºC to 500 ºC at the rate of 10 ºC min^{-1} in dynamic nitrogen atmosphere.

Results and discussion

Morphology characterization

The as-prepared DPD is polyhedron with the average particle size of 2 μm, as shown in **Fig. 2a** and **c**. The surface is slightly rough. **Fig. 2b** shows that one particle is aggregated by many nanodiamonds, and the open pores and defects are obviously observed on the surface. The specific surface area is 15.403 m^2 g^{-1} tested by

multipoint BET method. The X-Ray diffraction spectrum (see **Fig. 2d**) contains wide diffraction maxima at 2θ = 43.9°, 75.3° and 91.5° which correspond to the (111), (220) and (311) reflections of the diamond-like lattice. The strong peak of d = 2.06763 and the weak peak of d = 2.17821 represent the cubic crystal system and the hexagonal crystal system, respectively. Thus, DPD is composed of a large quantity of cubic diamonds and a small quantity of hexagonal diamonds. No graphite peak is detected in the region 2θ = 20~30°, which indicates that the formed powder is well-purified DPD.

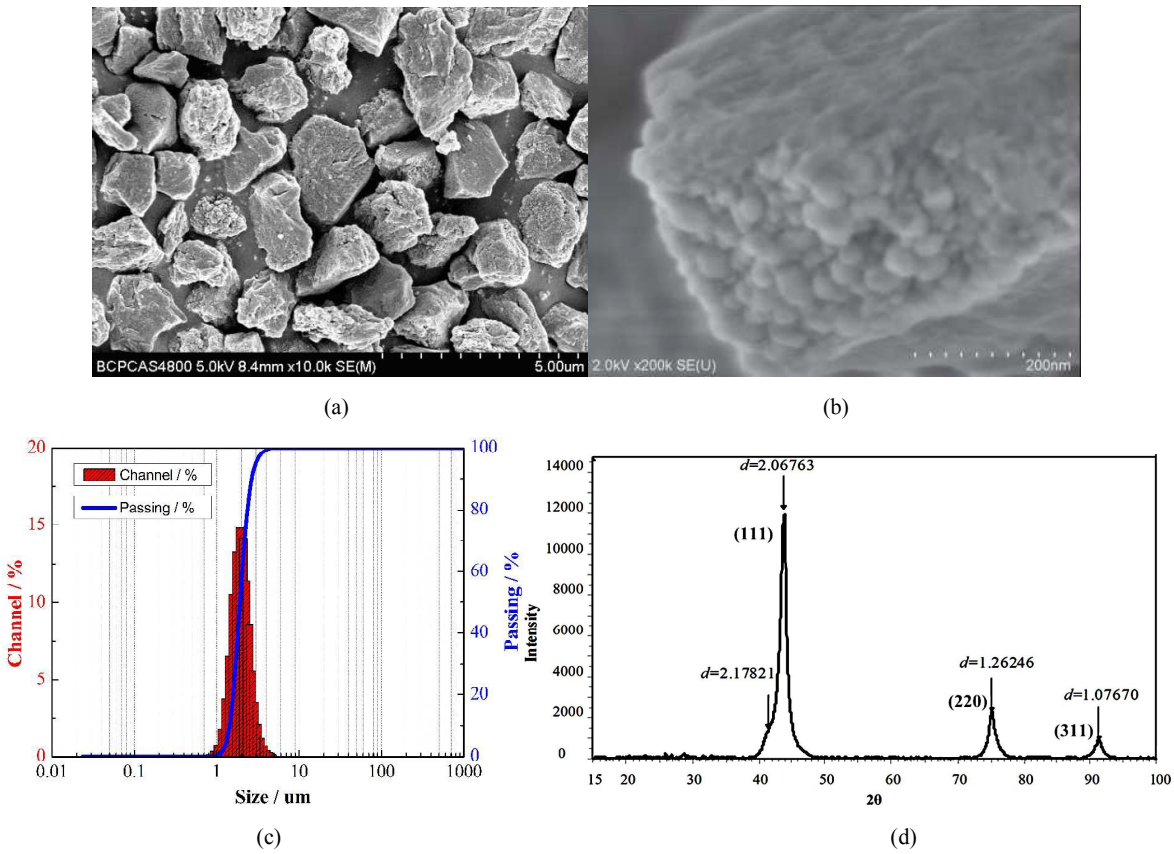

Fig. 2 Characteristics of DPD: (a)(b) SEM images of DPD powder and one particle; (c) particle size analysis; (d) powder-XRD image

RDX of the particle diameter of 100~150 μm is used as the substrate material for modification as shown in **Fig. 3a**. Its surface is comparatively smooth aside from a minute amount of fragments. DPD has much smaller particle size and large surface energy, and therefore has stronger surface attraction. It deposits and attaches on RDX surface via the intermolecular force under the effect of a surfactant Span-80. As shown in **Fig. 3b~e**, the

much rougher surfaces of DMRs indicate that DPD is successfully modified on RDX. Because no residue was detected after experiment, the efficient modified amounts of DMRs were reckoned by the ratios of DPD and RDX, which were DMR1 of 1/9, DMR2 of 1/7, DMR3 of 1/5 and DMR4 of 1/3.

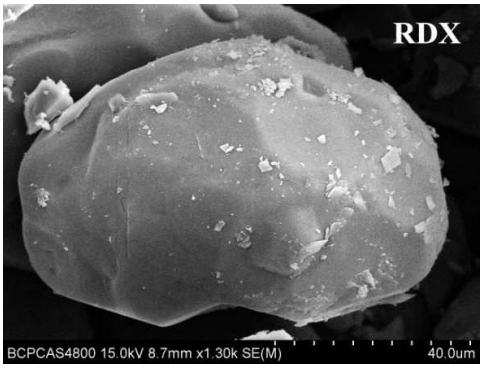

(a)

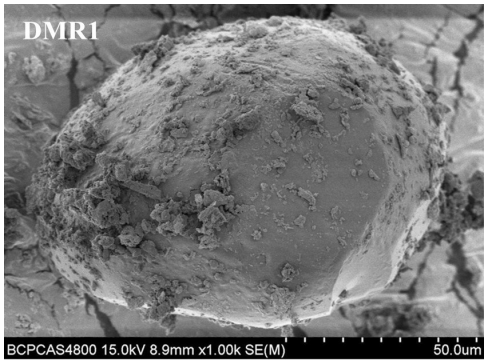

(b)

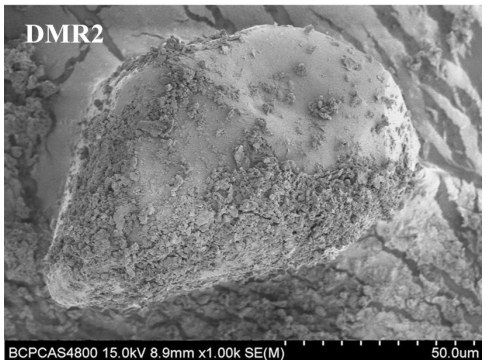

(c)

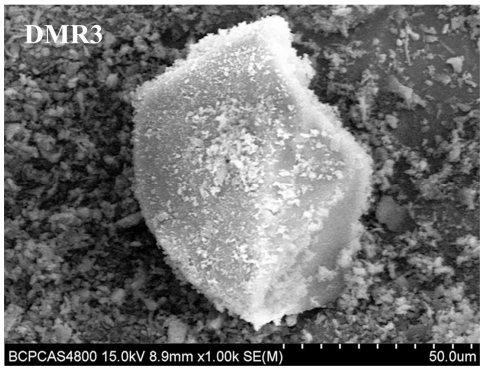

(d)

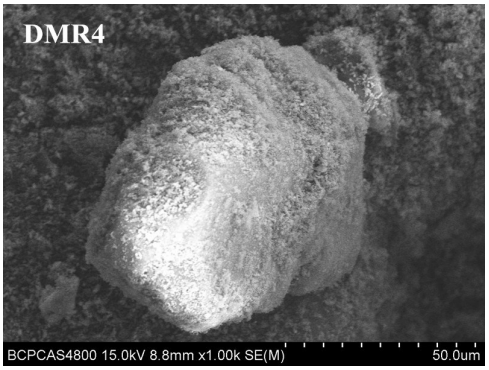

(e)

Fig. 3 SEM images of RDX and four DMRs

DPTA analysis

The gas emission of DPTA is used to evaluate the thermal stability of material; less gas emission signifies better

stability.[21, 22] DPTA was used to study the initial thermal decompositions of DMRs, recording the gas pressure of the thermal decomposition in real time and normalized at the standard condition of 1.0 g quantity, 25 mL volume and 273.15 K temperature, as shown in **Fig. 4**.

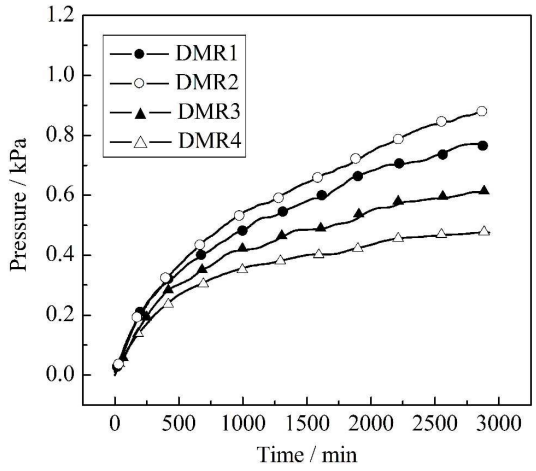

Fig. 4 Time dependences of decomposed gas pressures of DMRs at 100 °C recorded by DPTA

The gas emissions of all DMRs generally increase with the heating time lasting. The beginning 500 minutes is a fast decomposition period. The pressures increase rapidly and the increasing rates are arranged in an increasing order of DMR4 < DMR3 < DMR1 < DMR2. Subsequently, the decomposition turns into a slow period. The pressures continue to increase but the increasing rates decrease gradually in different degrees. They decompose and release gas slowly for a long duration. The thermal decompositions of DMRs do not reach equilibrium at the end of DPTA test (during 48 h). It implies that at the actual storage condition DMRs keep the slow steady decomposition for a long period of time until the equilibrium is established. The gas pressures are recalculated into the volumes and listed in **Table 1**.

Table 1 Gas emissions and reaction rate constants of DMRs from DPTA data [1]

Samples	Gas emission		Reaction rate constant		
	p / kPa g^{-1}	V / mL g^{-1}	k / 10^{-7}s^{-1}	b	r
DMR1	0.7696±0.0385	0.1899±0.0095	4.28	-0.01679	0.9952
DMR2	0.8854±0.0443	0.2185±0.0109	4.94	-0.07962	0.9934
DMR3	0.6097±0.0305	0.1505±0.0075	4.13	-0.00682	0.9955
DMR4	0.4694±0.0235	0.1158±0.0058	3.88	-0.00010	0.9982

[1] b—— intercept of the fitting plot of the solid phase reaction kinetic equation $G(\alpha) = k\alpha + b$; r—— linear correlation coefficient;

the most probability of *k* is selected according to the smallest value of *b* and the largest value of *r*.

Good thermal stability is required the gas emission less than 2.00 mL g^{-1} at 100 ºC during 48 h.[23, 24] The gas emissions of DMRs are all less than 2.00 mL g^{-1}, indicating that they have good thermal stability. The previous report on the DPTA gas emission of RDX is about 0.10 mL g^{-1}.[25] DMRs release more gas than RDX, thus the DPD modification is conducive to the decomposition of RDX. The total gas emission in an increasing order is DMR4 < DMR3 < DMR1 < DMR2. The DPD modification obviously affects the gas emission, but there is a non-linear correlation between the gas emission and the modified amount. The dependence of gas emission on modified amount shows a maximum value that corresponds to DMR2 with the modified amount of 1/7. The reaction rate constants (*k*) were calculated by the solid-phase reaction kinetic equation [26] and listed in **Table 1**. The *k* ranked in an increasing order is DMR4 < DMR3 < DMR1 < DMR2, which shows the same order as the gas emission. The reaction kinetics theory holds that *k* means the decrease of the concentration of reactant or the increase of the concentration of product in unit time. Due to the interactions among DPD, RDX and gaseous products, the moderate DPD modification could activate the reactant RDX to the greatest extent. On the microscopic level, the concentration of the activated reaction molecules and the chance of their effective collisions increase, and thus the reaction rate is accelerated. DMR2 of 1/7 modified amount has the fastest reaction rate and the most gas emission of DPTA within the specific time. Therefore, the moderate amount of DPD modification has the most efficient catalytic action, providing the greatest accelerating effect on the thermal decomposition of RDX.

DSC analysis

The nonisothermal decompositions of DMRs were recorded by DSC at the heating rate of 10 ^{o}C min^{-1}. The DSC curves are shown in **Fig. 5**.

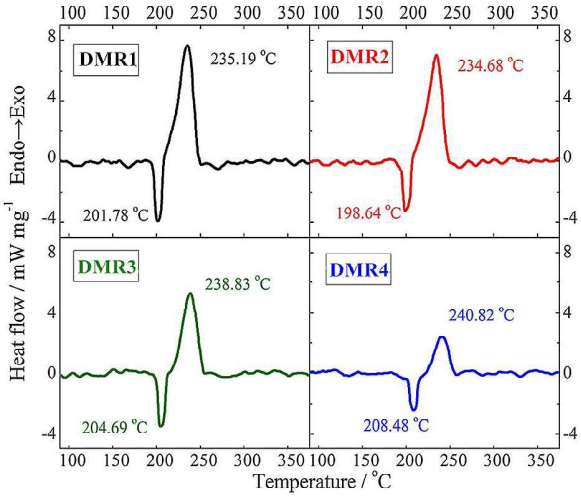

Fig. 5 DSC curves of DMRs at 10 °C min^{-1}

The DSC curves firstly show one endothermic peak caused by melting, immediately following one exothermic peak by intense thermal decomposition. DMRs decompose in molten state like RDX.[27] It indicates that DPD does not decompose but affects the decomposition of RDX. The detailed DSC data are summarized in **Table 2**.

Table 2 DSC parameters of DMRs at heating rate of 10 °C min^{-1} [1]

Samples	Melting endothermic peaks				Decomposition exothermic peaks			
	T_o / °C	T_p / °C	T_e / °C	ΔH_1 /J g^{-1}	T_o / °C	T_p / °C	T_e / °C	ΔH_2 /J g^{-1}
DMR1	180.40	201.78	213.14	-86.73	213.56	235.19	253.23	992.56
DMR2	180.06	198.64	206.33	-76.46	212.35	234.68	252.67	897.73
DMR3	184.66	204.69	207.62	-75.69	215.78	238.83	258.36	638.05
DMR4	186.35	208.48	215.01	-68.48	218.98	240.82	267.12	293.77

[1] T_o——onset temperature; T_p—— peak temperature; T_e—— end temperature; ΔH_1 and ΔH_2 —— enthalpy changes.

The pure RDX has the melting temperature of 205~208 °C and the decomposition temperature of 238~241°C.[28] After being modified by DPD, both the melting and decomposition temperatures of DMRs are lower than those of RDX. The DPD modification improves the decomposition of the composites. As shown in **Table 2**, all the characteristic temperatures of the thermal decomposition increase in an order of DMR2 < DMR1 < DMR3 < DMR4. DMR2 of 1/7 modified amount has the lowest decomposition temperatures and thus the highest reaction activity. However, the enthalpy changes of endothermic and exothermic decompositions

(ΔH_1 and ΔH_2) conform to the order of DMR4 < DMR3 < DMR2 < DMR1. The heat change is caused by the decomposition of RDX, therefore ΔH_1 and ΔH_2 are in direct proportion to the content of RDX.

TG/DTG analysis

The thermal decompositions of DMRs at different heating rates were studied by TG, and the mass losses and their differential curves are shown in **Fig. 6**. The characteristic parameters of TG/DTG curves are listed in **Table 3**.

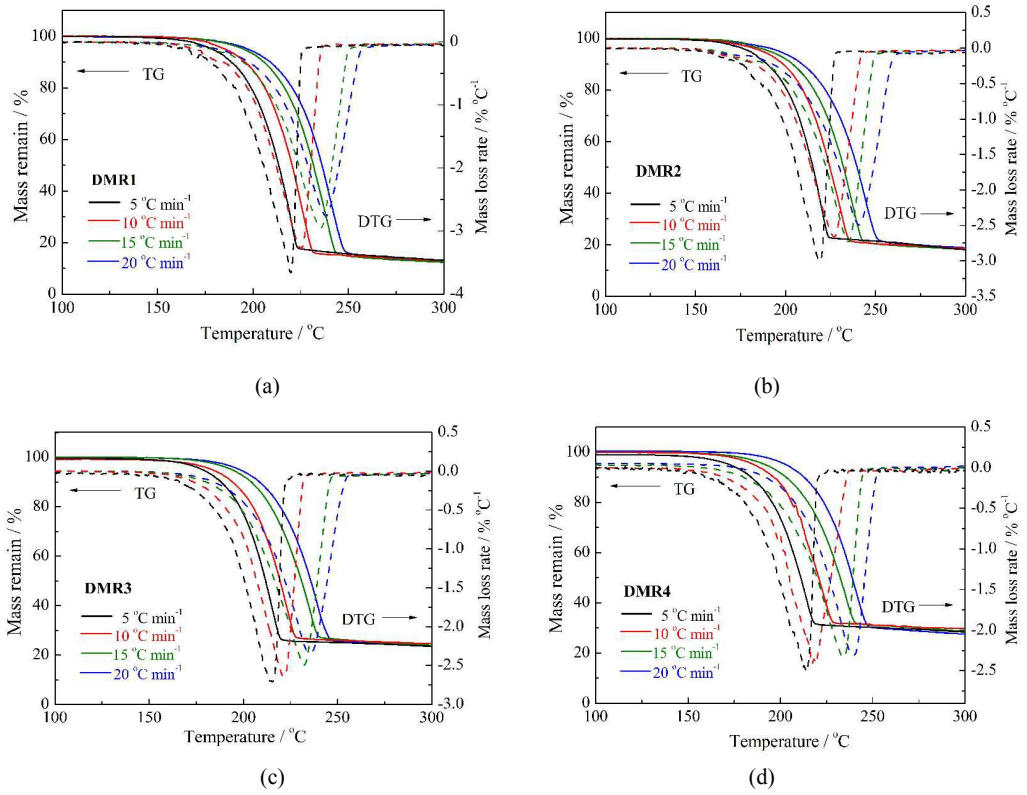

Fig. 6 TG/DTG curves of DMRs

The thermal decompositions of all DMRs show only one intense mass loss process. They decompose completely because their loss masses are in good agreement with the amounts of RDX and the residues are almost the unreacted DPD. Both the peak temperature of thermal decomposition (T_p) and the maximum mass loss rate (Δm_{max}) increase with the increase of heating rate. The critical temperature of thermal explosion (T_b) and self-accelerating decomposition temperature (T_{SADT}) [29, 30] are calculated (see **Table3**) to predict the thermal

safety of DMRs.

Table 3 Characteristic parameters of DMRs from non-isothermal TG/DTG data [1]

Samples	Curve parameters			Characteristic temperatures	
	β / °C min^{-1}	T_p / °C	Δm_{max} / % min^{-1}	T_b / °C	T_{SADT} / °C
DMR1	5.0	220.21	18.84	227.75	210.12
	10.0	225.03	34.38		
	15.0	237.55	47.05		
	20.0	240.48	62.39		
DMR2	5.0	220.44	17.32	219.27	205.68
	10.0	230.05	28.99		
	15.0	236.84	44.85		
	20.0	237.70	58.25		
DMR3	5.0	215.41	16.24	222.23	203.55
	10.0	222.91	28.48		
	15.0	234.43	41.96		
	20.0	238.79	55.88		
DMR4	5.0	218.14	14.39	224.63	205.27
	10.0	222.64	27.58		
	15.0	238.04	39.93		
	20.0	238.65	55.18		

[1] β—— heating rate; T_p—— peak temperature of mass loss rate; Δm_{max}—— maximum mass loss rate; T_b—— critical temperature of thermal explosion, $T_p=T_{p0}+a\beta+b\beta^2$, $T_b=[E_a-(E_a^2-4E_aRT_{p0})^{1/2}]/2R$; T_{SADT}—— self-accelerating decomposition temperature, $T_{SADT}=T_b-(RT_b^2/E_a)$.

Higher characteristic temperature denotes better thermal safety. T_b is ranked in an increasing order of DMR2 < DMR3 < DMR4 < DMR1 while T_{SADT} is DMR3 < DMR4 < DMR2 < DMR1. No identical variation is shown in the temperatures due to the complex interactions between RDX and DPD. The best thermal safety belongs to the composite with the modified amount of *ca.* 1/7.

The thermodynamic parameters of thermal decompositions of DMRs were calculated based on the transition state theory and the kinetic parameters were calculated by Kissinger and Ozawa methods.[26] All the parameters are summarized in **Table 4**.

Table 4 Thermodynamic and kinetic parameters of DMRs from non-isothermal TG [1]

Samples	Thermodynamic parameters			Kinetic parameters				
				Kissinger method			Ozawa method	
	$\Delta H^{\neq}$ / kJ mol^{-1}	$\Delta S^{\neq}$ / J K^{-1} mol^{-1}	$\Delta G^{\neq}$ / kJ mol^{-1}	E_{aK} / kJ mol^{-1}	lg(A_K / s^{-1})	$-r_K$	E_{aO} / kJ mol^{-1}	$-r_O$
DMR1	112.02	-65.10	143.48	116.04	10.04	0.9505	118.31	0.9565

DMR2	143.68	-0.60	143.94	147.64	13.40	0.9866	148.33	0.9879
DMR3	102.60	-83.15	142.24	106.56	9.09	0.9778	109.24	0.9808
DMR4	99.60	-90.05	142.68	103.57	8.73	0.9257	106.43	0.9354

[1] $\Delta H^{\neq}$—— enthalpy of activation, $\Delta H^{\neq}=E_a-RT$; $\Delta S^{\neq}$—— entropy of activation, $\Delta S^{\neq}=R[\ln A-\ln(k_BT/h)]$; $\Delta G^{\neq}$—— free energy of activation, $\Delta G^{\neq}=\Delta H^{\neq}-T\Delta S^{\neq}$; E_a—— apparent activation energy; A—— pre-exponential factor; r—— linear correlation coefficient; the subscript K and O indicate the parameters were calculated by Kissinger and Ozawa methods, respectively.

The thermodynamic and kinetic parameters are ranked in the same order of DMR4 < DMR3 < DMR1 < DMR2. The transition state theory and the collision theory hold that A closely relates to $S^{\neq}$, because both parameters represent the confusion degree and collision probability of the reaction molecules.[31, 32] Due to the higher chemical activity, the micro- and nano materials have greater confusion degree and collision probability than the larger-sized counterparts. Therefore, for the micro- and nano materials, the A plays a dominate role in determining the feasibility and activity of the reaction involving the catalysis. This conclusion has also been confirmed by our earlier research.[33] DMR2, corresponding to the modified amount of 1/7, has the largest value of A and therefore the highest reactivity.

The direct proportion between E_a and A indicates that the kinetic compensation effect lies in the thermal decomposition of DMRs.[34] It suggests that their decompositions have the same rate-determining reaction step.[30] The different quantities of DPD modification could change some reaction pathways and affect the thermal decomposition kinetics, but not change the rate-determining step. Therefore, all DMRs have the same rate-determining step as RDX. The previous researches have concluded that the rate-determining step of thermal decomposition of RDX is the scission of one of the N-NO_2 bonds (see **Scheme 1**).[36-39] Likewise, this step dominates the decomposition of DMRs.

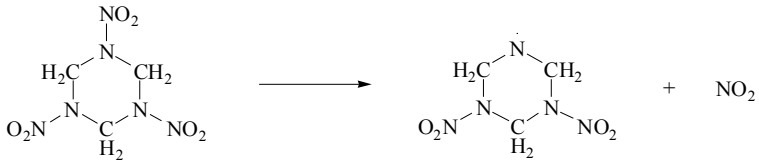

Scheme 1 Rate-determining step of thermal decomposition of RDX: the scission of N-NO_2 bond.

Isoconversional kinetic analysis

The isoconversional principle states that the reaction rate at constant extent of conversion is only a function of

temperature. The temperature dependence of the isoconversional rate can be used to evaluate the isoconversional values of activation energy (E_α) without assuming or determining any particular form of the reaction model.[40] The E_α dependence is important for detecting and treating the multistep kinetics. A significant variation of E_α with extent of conversion (α) indicates that a reaction is a kinetically complex multi-step process.[41, 42] Although the isoconversional principle holds strictly for a single-step process, the principle continues to work as a reasonable approximation because the isoconversional methods describe the process kinetics by using multiple single step kinetic equations. The International Confederation for Thermal Analysis and Calorimetry (ICTAC) Kinetics Committee recommends the Kissinger-Akahira-Sunose (KAS) equation to calculate the isoconversional activation energy E_α.[40]

KAS equation:
$$\ln\left(\frac{\beta_i}{T_{\alpha,i}^2}\right) = \text{Const} - \frac{E_\alpha}{RT_{\alpha,i}} \quad (i = 1, 2, 3, 4) \tag{1}$$

where the subscript α indicates isoconversional value, β_i is heating rate of TG, $T_{\alpha,i}$ is the temperature corresponding to a given conversion value at different β_i. Firstly, the α vs. T curves of four DMRs are plotted in **Fig. 7**.

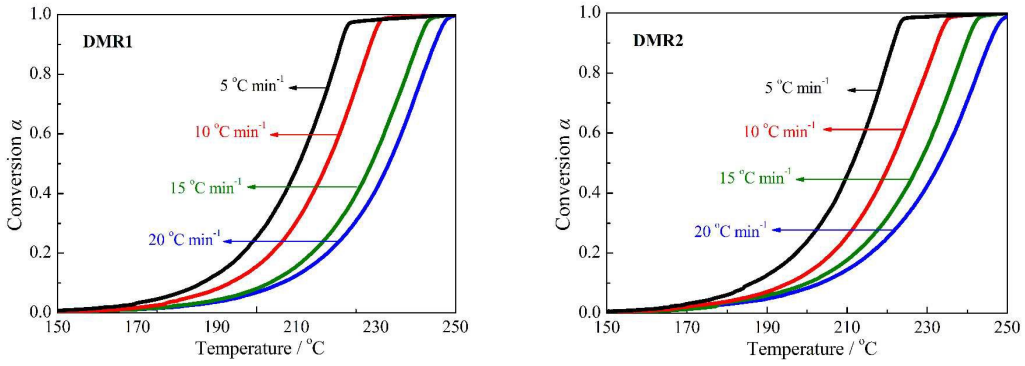

(a) (b)

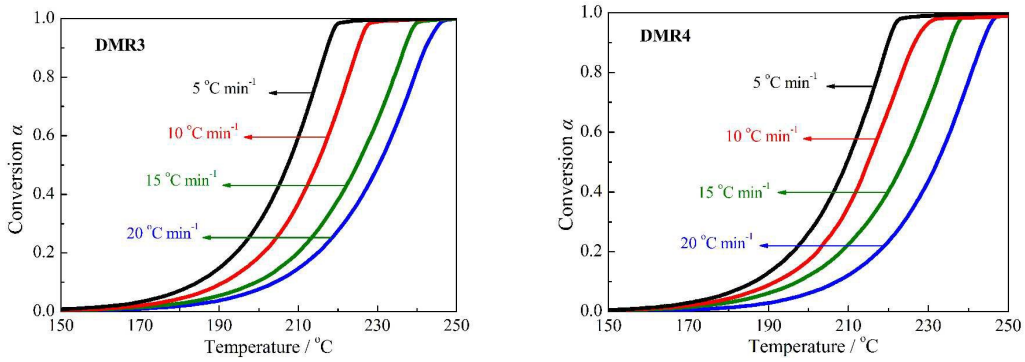

(d) (d)

Fig. 7 α vs. T curves of DMRs under different heating rates

All of the curves obey the similar sigmoidal trend. It shows that the thermal decomposition process of DMRs is subdivided into three stages i.e. the lag, acceleration and deceleration stage. The value of E_α is determined from the slope of the plot of ln $(\beta_i/T_{\alpha,i})$ vs. $1/T_{\alpha,i}$ as shown in **Eq.(1)**. The values of E_α at different α are listed in **Table 5.**

Table 5 Isoconversional kinetic parameters of DMRs by KAS method

α	DMR1		DMR2		DMR3		DMR4	
	E_α / kJ mol^{-1}	$-r$	E_α / kJ mol^{-1}	$-r$	E_α / kJ mol^{-1}	$-r$	E_α / kJ mol^{-1}	$-r$
0.1	110.58±15.59	0.9807	152.01±18.77	0.9851	118.41±14.02	0.9863	104.97±25.36	0.9463
0.2	109.37±15.27	0.9811	149.06±16.09	0.9886	115.25±14.25	0.9849	104.83±23.02	0.9550
0.3	108.84±16.03	0.9790	142.51±13.40	0.9913	112.56±14.79	0.9832	102.95±24.04	0.9496
0.4	106.94±16.81	0.9762	139.69±13.13	0.9913	110.13±15.63	0.9805	100.60±25.22	0.9425
0.5	108.62±16.57	0.9775	136.35±13.08	0.9910	108.04±15.57	0.9799	96.93±26.07	0.9347
0.6	109.78±17.08	0.9766	133.51±11.38	0.9928	106.08±15.12	0.9803	97.29±26.09	0.9350
0.7	109.24±17.54	0.9752	132.39±11.38	0.9927	103.62±15.63	0.9780	97.08±25.66	0.9367
0.8	108.99±17.61	0.9749	131.47±12.26	0.9914	103.34±15.62	0.9779	98.17±24.63	0.9424
0.9	108.19±16.86	0.9766	130.68±11.26	0.9927	101.40±15.62	0.9771	100.21±22.79	0.9520
Mean	108.95±16.60		138.63±13.42		108.76±15.15		100.34±24.77	
SD[1]	0.9631		7.3704		5.4694		3.0693	

[1] SD—— standard deviation.

The E_α vary with the α, thus the decomposition of DMR can be described as a multi-step process. For the energetic explosives, the thermal decomposition process includes one slow initial decomposition step and one rapid autocatalytic decomposition step, and the latter is caused by the secondary reactions between the reactants and products. Therefore, the decomposition of DMR includes at least two kinds of accelerating reactions; they

are the autocatalytic reaction caused by their own gaseous products and the catalytic reaction by the DPD modification. As shown in **Fig. 8**, the change trends of E_α vs. α of DMRs are different from each other. It shows that the effect of DPD modification on the reaction mechanism varies with the modified amount. According to the standard deviation (SD), DMR2 has the greatest change of E_α vs. α, so the modified amount of 1/7 has the greatest effect on the thermal decomposition of RDX. Although all DMRs have the same rate-determining step, DPD modification change the reaction pathway and reaction rate and then affect the reaction mechanisms and kinetics.

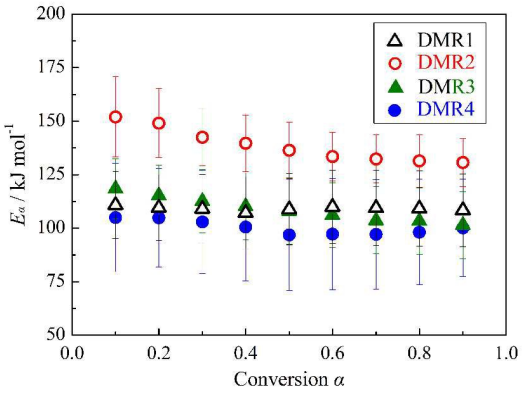

Fig. 8 Dependences of E_α vs. α by KAS method

DPD-modified effect

The characteristic parameters of the thermal decomposition of DMRs are not in direct proportion to the DPD modified amount. The DPD-modified effect on thermal decomposition of RDX can be illustrated in **Fig. 9**.

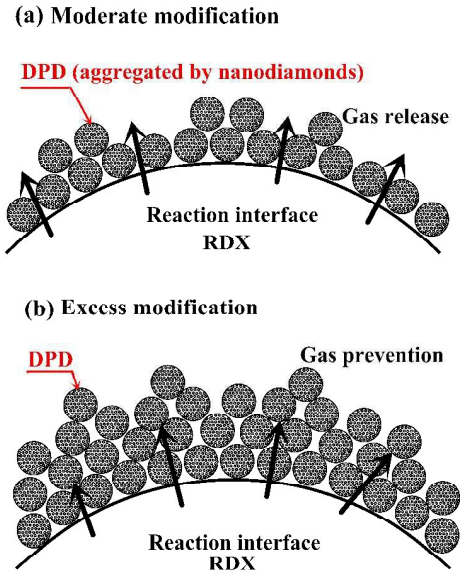

Fig. 9 Effect of DPD modification on thermal decomposition of RDX

DPD has high activity due to their small size, large surface and fast heat & mass transfer. It also has many open pores and defects on the surfaces (see **Fig. 2b**) which are available for the active sites of reaction and the potential attached sites of the active hydrogen. The gaps between the aggregated nanoparticles are the diffusion path for the gaseous products. These factors arouse the catalysis of DPD on the thermal decomposition. As the modified amount increases from 0 to 1/7, the concentration of activated molecules increases, and the probability of reactive collisions between DPD, RDX and gaseous products increases, thus the catalytic activity become higher. Consequently, the DPD modification leads to lower decomposition temperature, faster reaction rate and more gas emission within a given time. However, when the modified amount exceeds 1/7, excess DPD modification hinders the diffusion of gaseous products and decreases the activity of the reaction interface of RDX, and thus has a negative effect on the thermal decomposition of RDX.

Conclusions

DPD of the particle size of 2 μm was prepared from graphite through direct detonation preparation. DPD were modified on the micron RDX particles, preparing four DMR composites. The effect of DPD modification on the thermal decomposition of RDX was studied by DSC, TG and DPTA techniques. The thermal stability was

ranked in an order of DMR4 < DMR3 < DMR1 < DMR2. The similar change trends were found in the gas emission, decomposition temperature, kinetic and thermodynamic parameter with increasing modified amount. DMR2 with the modified amount of 1/7 reached the extreme values of the decomposition characteristic parameters and improve the thermal property of RDX to the greatest extent. The catalysis of the DPD modification was not linearly proportional to the modified amount. A moderate amount of DPD modification as a catalyst accelerated the decomposition, while excess modification conversely obstructed the decomposition. The thermal decomposition kinetics indicated that the thermal decompositions of DMRs had the same rate-determining step, i.e. the scission of one of the N-NO_2 bonds of RDX, and conformed to the multi-step reaction mechanism involving the catalytic reaction and secondary reaction.

Acknowledgements

This work was financially supported by the Science and Technology Fund on Applied Physical Chemistry Laboratory (Nos. 9140C3703051105 and 9140C370303120C37142), and the Key Support Foundation of State Key Laboratory of Explosion Science and Technology (Nos. QNKT12-02 and YBKT 10-05).

References

1. A. V. Kurdyumov, O. N. Breusov, V. N. Drobyshev, V. A. Melnikova and V. F. Tatsii, *Combust. Explo. Shock*, 1989, **25**, 380-382.
2. T. Jiang and K. Xu, *Carbon*, 1995, **33**, 1663-1671.
3. V. M. Titov, V. F. Anisichkin and I. Y. Malkov, *Combust. Explo. Shock*, 1989, **25**, 372-379.
4. A. L. Vereschagin, G. V. Sakovich, V. F. Komarov and E. A. Petrov, *Diam. Relat. Mater.*, 1994, **3**, 160-162.
5. O. R. Bergmann, N. F. Bailey and H. B. Coverly, *Metallography*, 1982, **15**, 121-139.
6. Y. Nakamura, H. Sato, M. Ohtsuka and S. Hojo, *Bio-Med. Mater. Eng.*, 2010, **20**, 283-293.
7. W. Du, S. Wei, K. Zhou, J. Guo, H. Pang and X. Qian, *Mater. Res. Bull.*, 2015, **61**, 333-339.
8. C.H. Wang, Z.S. Guo, F. Pang, L.Y. Zhang, M. Yan, J.H. Yan, K.W. Li, X.J. Li, Y. Li, L. Bi and Y.S. Han, *ACS Appl. Mater. Interfaces*, 2015, **7**, 15263–15276.
9. L.M. Dai, M. Awh, *Adv. Mater.*, 2001, **13**, 899-899.
10. A. Burakov, I. Romantsova, A. Kucherova and A. Tkachev. *Adsorpt. Sci. & Technol.*, 2014, **32**, 737-747.
11. Y. Tong, R. Liu and T.L. Zhang, *Phys. Chem. Chem. Phys.*, 2014,**16**, 17648-17657.
12. M. Fathollahi, B. Mohammadi and J. Mohammadi, *Fuel*, 2013, **104**, 95-100.
13. V. Strunin and L. Nikolaeva, *Combust. Explo. Shock*, 2013, **49**, 53-63.

14. D. M. Badgujar, M. B. Talawar, S. N. Asthana and P. P. Mahulikar, *J. Hazard. Mater.*, 2008, **151**, 289-305.
15. T. M. Klapotke and G. Steinhauser, *Angew. Chem. Int. Ed.*, 2008, **47**, 3330-3347.
16. M. B. Talawar, R. Sivabalan, T. Mukundan, H. Muthurajan, A. K. Sikder, B. R. Gandhe and A. S. Rao, *J. Hazard. Mater.*, 2009, **161**, 589-607.
17. X. Qi, X. Zhang, Q. Yan, Z. Song, P. Liu and J. Li, *Chem. Propel. Polym. Mater.*, 2012, **1**, 016.
18. C. Hou, X. Geng, C. An, J. Wang, W. Xu and X. Li, *Cent. Eur. J. Energ. Mater.*, 2013, **10**.
19. Y. L. Zhu, H. Huang, H. Ren and Q. J. Jiao, *J. Energ. Mater.*, 2013, **31**, 178-191.
20. R. Liu, Z. Zhou, Y. Yin, L. Yang and T. Zhang, *Thermochim. Acta*, 2012, **537**, 13-19.
21. R. Liu, T. Zhang, L. Yang and Z. Zhou, *Cent. Euro. J. Chem.*, 2014, **12**, 672-677.
22. R. Liu, L. Yang, Z. Zhou and T. Zhang, *J. Therm. Anal. Calorim.*, 2014, **115**, 1939-1948.
23. GJB 772A-97. Method 501.2: Vacuum stability test - Method of pressure transducer. Commission of Science, Technology and Industry for National Defense. Beijing, 1997. pp. 156-158.
24. GJB 5891.12 - 2006. Test method of loading material for initiating explosive device - Part 12: Vacuum stability test - Method of pressure transducer. Commission of Science, Technology and Industry for National Defense. Beijing, 2006. pp. 67-70.
25. Y.L. Yin, L. Yang, X.C. Hu, Z.M. Li, K.Y. Li, T.L. Zhang and J.G. Zhang, *Chin. J. Energ. Mater.*, 2010, **18**, 387-392.
26. R. Z. Hu, S. L. Gao, F. Q. Zhao, Q. Z. Shi, T. L. Zhang and J. J. Zhang, Thermal Analysis Kinetics second ed, Science Press, Beijing, 2008.
27. G. Hussain and G. J. Rees, *Fuel*, 1995, **74**, 273-277.
28. J. S. Lee, C. K. Hsu and C. L. Chang, *Thermochim. acta*, 2002, **392**, 173-176.
29. J. Yi, F. Zhao, B. Wang, T. An, Y. Wang and H. Gao, *J. Therm. Anal. Calorim.*, 2014, **115**, 1227-1234.
30. B. Yan, H. X. Ma, N. N. Zhao, T. Mai, J. R. Song, F. Q. Zhao and R. Z. Hu, *J. Therm. Anal. Calorim.*, 2012, **110**, 1253-1257.
31. K. Morokuma, B. C. Eu and M. Karplus, *J. Chem. Phys.*, 1969, **51**, 5193-5203.
32. P. Pechukas and F. J. McLafferty, *J. Chem. Phys.*, 1973, **58**, 1622-1625.
33. R. Liu, W. Yu, T. Zhang, L. Yang and Z. Zhou, *Phys. Chem. Chem. Phys.*, 2013, **15**, 7889-7895.
34. A. K. Galwey and M. Mortimer, *Int. J. Chem. Kinet.*, 2006, **38**, 464-473.
35. J. G. R. Poco, H. Furlan and R. Giudici, *J. Phys. Chem. B*, 2002, **106**, 4873-4877.
36. H. W. Liu and R. N. Fu, *Thermochim. Acta*, 1989, **138**, 167-171.
37. C. A. Wight and T. R. Botcher, *J. Am. Chem. Soc.*, 1992, **114**, 8303-8304.
38. T. R. Botcher and C. A. Wight, *J. phys. Chem.*, 1994, **98**, 5441-5444.
39. A. A. Zenin and S. V. Finjakov, *Combust. Explo. Shock*, 2009, **45**, 559-578.
40. S. Vyazovkin, A. K. Burnham, J. M. Criado, L. A. Perez-Maqueda, C. Popescu and N. Sbirrazzuoli, *Thermochim. Acta*, 2011, **520**, 1-19.
41. S. Vyazovkin and N. Sbirrazzuoli, *Macromol. Rapid Comm.*, 2006, **27**, 1515-1532.
42. W. Wu, J. Cai and R. Liu, *Ind. Eng. Chem. Res.*, 2013, **52**, 14376-14383.

Effect of detonation polycrystalline diamond modification on thermal decomposition of RDX

Yi Tong, Rui Liu and Tonglai Zhang

Graphical Abstract

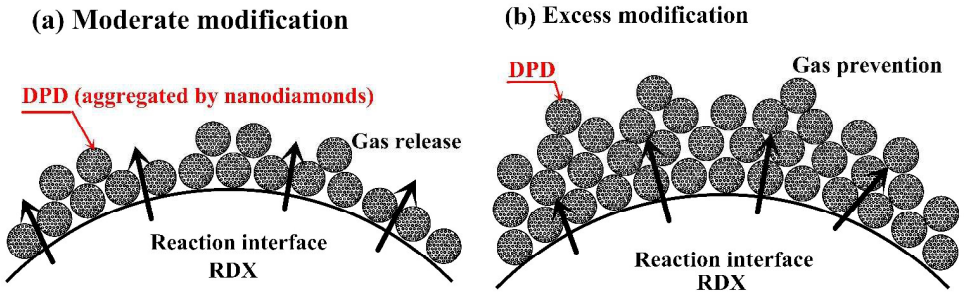

A moderate amount of DPD modification as a catalyst accelerated the decomposition, while excess modification conversely obstructed the decomposition.